MIJST
MIST International Journal of Science and Technology

Evaluation of Physical, Mechanical, and Durability Properties of Limestone Powder Blended Concrete

Md. Jahidul Islam, Tasnia Ahmed*, Nishat Naila Meghna, Ismat Abida, and Nayeem Mohammad Mashfiq

Department of Civil Engineering, Military Institute of Science and Technology, Dhaka, Bangladesh

***Corresponding Email:** *tasnia@ce.mist.ac.bd*

ARTICLE INFO

Article History:

Received: 13th July 2025
Revised: 29th September 2025
Accepted: 06th October 2025
Published: 30th December 2025

Keywords:

Blended cement concrete
Limestone powder
Tensile strength prediction
Flexural strength
Durability

ABSTRACT

Reducing the amount of cement in construction has become a challenge in the 21st century. In this study, limestone powder (LSP) is adopted to partially replace cement at different weight percentages (5%, 10%, 15% and 20%). The influence of LSP on engineering properties such as workability, compressive strength, splitting tensile strength, flexural strength and toughness, water permeability, and surface resistivity is investigated to assess the acceptability of LSP blended concrete and to find the optimum replacement level considering these properties. At low replacement levels (5% and 10%), the mechanical and durability properties are improved due to the nucleation effect of LSP. Beyond 10% replacement, the dilution effect dominates which disadvantages the concrete. The workability linearly rises with the increase in the LSP content. The compressive and tensile strength does not vary much from the control specimen up to a 10% replacement level. The highest compressive and flexural strength is recorded for 10% LSP replacement. Toughness calculated from the beam load-deflection curve showed an increased value with increased LSP replacement. In comparison to the control specimens, 6.4% higher flexural strength and 90% higher toughness index are achieved for 10% LSP. An equation has been proposed using a machine learning approach to predict the tensile strength of LSP blended concrete with 87% accuracy. Water permeability and chloride ion penetrability are reduced for higher LSP content as LSP works as a filler and enhances pore structure. This study summarizes that 10% cement substitution with the LSP can be adopted for overall better mechanical and durability properties of concrete.

1. INTRODUCTION

Concrete is a multi-component and versatile composite material. It is used at a much higher rate today on account of the expanding population and urbanization. Concrete manufacturing has put a lot of pressure on the atmosphere. The global cement production, a key component of concrete, has been increasing steadily, reaching over 4.3 billion tons in 2022 (Barbhuiya *et al.*, 2024). The annual cement supply accounts for around 7-8% of global CO_2 emissions, hence contributing significantly to climate change and the greenhouse effect (Amran *et al.*, 2022).

Over the last few decades, using various byproducts in concrete production has become a common practice. Natural pozzolans, silica fume, slag, fly ash, and limestone powder can be used as cementing materials (Meghna *et al.*, 2025; T. Ahmed *et al.*, 2024; Islam *et al.*, 2023a; Islam *et al.*, 2023b; P. P. Li *et al.*, 2020; EN, 2000; T. Ahmed *et al.*, 2025; Araf *et al.*, 2023). The use of such materials reduces the environmental impact of Portland cement manufacturing, conserves natural resources, and increases concrete's mechanical and durability properties (Meddah *et al.*, 2014). Limestone powder (LSP), a byproduct of limestone quarry, has long been utilized in cement-based products. It is natural and readily available at a low cost. Various standards allow LSP applications in cement manufacturing (ASTM C150, 2022; ACI 211.7R-15, 2015). Additionally, structures made with LSP as cement substitution are proven to produce 30% less CO_2 than traditional concrete (Barbhuiya *et al.*, 2023).

LSP exhibits limited pozzolanic activity due to its primary composition of calcium carbonate ($CaCO_3$), which does not readily react with calcium hydroxide (CH) to form additional calcium silicate hydrate (C-S-H) gel. (Liu & Yan, 2010). Although the pozzolanic activity of LSP is minimal, its role in refining concrete microstructure can positively influence the mechanical properties through its micro-filler effect, particle packing, and reducing porosity over time (Zhao *et al.*, 2024; Mahi *et al.*, 2025).

P. P. Li *et al.* (2020) substituted LSP with binder by 0 to 80% volume. Their results indicate that even though a high volume of LSP produces cost-effective and eco-friendly concrete, a 50% LSP replacement level appeared to be the optimum, considering the compressive strength, porosity, and binder efficiency. Gesoğlu *et al.* (2012) found that for 5%, 10% and 20% LSP, the compressive strength increased respectively by 8%, 5% and 7% compared to control cylinders. Their study suggests a 10% LSP replacement level to be the optimum percentage. Vance *et al.* (2013) illustrated the workability of concrete replacing cement with LSP up to 40% and using different particle sizes of LSP. With the increase in the percentage of LSP, the workability of concrete decreased. LSP has a filler effect here, and as particle size grows, plastic viscosity and yield stress drop, reducing the workability of concrete.

Lothenbach *et al.* (2008) found that the early compressive strength decreases with a large volume of LSP; however, it increases with concrete age. On the other hand, Celik *et al.* (2019) found that the control sample, which contains no replacement of cement, showed higher strength than the sample containing 15% replacement of cement at 1 day and 3 days, respectively. However, the strength of concrete having 15% LSP was just 2% lower after 7 days. Although this is an excellent early age strength growth, the concrete containing a 15% LSP mixture provided 15% less strength than the concrete containing no LSP content after 91 days of hydration. According to Dhir *et al.* (2007), regardless of curing age, there was a consistent decrease in compressive strength test results with increasing LSP content.

Moreover, Demirhan *et al.* (2019) observed that the reduction in mortar compressive strength was 14%, 22%, and 28% for LSP replacement of 15%, 25%, and 35%, respectively, compared to the no replacement mortar at 28 days. The study indicated that LSP content greater than 15% did not continue hydration processes, leading to intensified matrices with reduced compressive strength. Tensile strength also decreases in the presence of LSP. Q. Wang *et al.* (2017) demonstrated that the splitting tensile strength of concretes containing LSP stayed virtually constant (within a limited fluctuation range) from 1 to 5 years. In contrast, plain cement concrete showed increased strength over the same period. Mohammed and Al-Numan (2024) found that replacing cement with 15% or 20% LSP reduced the 28-day splitting tensile strength by 39%, compressive strength by 71%, and flexural strength by 43% compared to the samples without LSP.

The addition of LSP can reduce porosity and pore size of concrete up to a certain replacement level. Several studies have demonstrated that using up to 8-10% LSP as a cement replacement can lower the water permeability of concrete (Lin *et al.*, 2020; L. G. Li & Kwan, 2015; Jiajian Chen *et al.*, 2014). JJ Chen *et al.* (2014) observed that, at the same w/c ratio, the water penetration depth decreased as the volume of LSP increased. This effect of LSP was generally more significant at higher w/c ratios. They observed that with 8% limestone filler added as cement paste replacement, the water penetration depth was reduced by 40 %, 59 %, and 61% at w/c ratios of 0.4, 0.5, and 0.6, respectively. When a small proportion of fine LSP was used to replace cement, it essentially functioned as a filler material and reduced the concrete's chloride permeability. The chloride permeability of the concrete was lowered when LSP substitution was less than 20% (Gesoğlu *et al.*, 2012). However, according to Meddah *et al.* (2014), up to 15% LSP did not affect the chloride diffusion coefficients. LSP also minimizes shrinkage by reducing the w/c ratio and improving internal curing, which lessens the overall volume change during drying and hardening (Ratsarahasina *et al.*, 2022).

The inclusion of LSP has several advantages, including reduced hydration heat, improved workability, lower CO_2 emissions, and improved concrete sustainability (X.-Y. Wang, 2020). Based on the literature review, different researchers used various percentages of LSP to find several mechanical properties. However, none of the reported studies performed an extensive study to find the various physical, mechanical, and durability characteristics and suggested an optimum LSP percentage. Thus, the objective of this study is to investigate the optimum content of LSP to get the best possible result while considering numerous physical, mechanical, and durability properties of concrete. Four different volumetric replacement percentages, such as 5%, 10%, 15%, and 20% have been considered in this regard to assess the application of LSP as a cement substitute in concrete.

2. EXPERIMENTAL INVESTIGATION

2.1 Materials

Ordinary Portland cement (OPC) is used as the binding material in this study. Limestone powder (LSP) is used to replace OPC partially. For this purpose, LSP was collected from a quarry in the United Arab Emirates through a local company. Figure 1 shows the pictures of OPC and LSP. The pictures show that OPC has a greyish colour, whereas LSP has a white colour. The compressive strength of the cement mortar was determined following the ASTM C109 [25]. Mortar compressive strength was 22 MPa, 27 MPa, and 37 MPa at 3, 7, and 28 days, respectively. Other physical tests of OPC and LSP were performed following the standard methods and are presented in Table 1. Chemical analysis of OPC and LSP was also performed and shown in Table 2. The test results indicate that OPC has a good amount of calcium oxide (CaO) and LSP has a high calcium carbonate ($CaCO_3$) content with a pH of 6-9.

(a) (b)

Figure 1: Concrete Ingredients: (a) Cement and (b) Limestone powder.

Table 1: Physical Properties of OPC and LSP

Property	Normal consistency	Specific gravity	Fineness	Initial setting time	Final setting time
Standard	ASTM C187 (2023)	ASTM C188 (2023)	ASTM C204 (2024)	ASTM C191 (2021)	
OPC	28%	3.15	397 m^2/kg	195 min	240 min
LSP	-	2.90	480 m^2/kg	-	-

Table 2: Chemical composition of OPC and LSP

Compound	% mass	
	OPC	LSP
$CaCO_3$	-	98.4
CaO	61.24	-
SiO_2	23.14	0.03
Al_2O_3	6.58	0.02
Fe_2O_3	2.69	0.02
SO_3	2.56	-
MgO	1.52	0.02
K_2O	0.70	-
Na_2O	0.21	-
LOI	1.36	-
Moisture	-	0.10

Locally available Sylhet sand with a nominal maximum size of 4.75 mm was used. It is a moderately coarse fine aggregate with a fineness modulus (FM) of 2.73. The adopted coarse aggregate had a maximum grain size of 19 mm with FM 6.85. The gradation curve of fine aggregate is depicted in Figure 2, which falls within the ASTM C33 (2023) defined range for fine aggregate used for concrete.

2.2 Mixture Proportions and Specimens

Five distinct concrete mixes are prepared for this investigation to assist in the comparative analysis. Concrete mix proportion was performed following the ACI 211.1 (1991) with a constant w/c ratio of 0.45. The water content was kept constant at 205 kg/m^3. Based on the literature review, it was revealed that the mechanical and durability properties of LSP blended cement concrete would decrease with the increase in LSP content. Studies suggest that different LSP content is optimum for different properties based on the curing age (Celik *et al.*, 2019; Pliya & Cree, 2015; Gesoğlu *et al.*, 2012). On the other hand, LSP content greater than 15% averts the hydration processes (Demirhan *et al.*, 2019). Therefore, a maximum of 20% of OPC is replaced with LSP. To find the optimum LSP percentage to achieve the best result while considering physical, mechanical, and durability properties of concrete, four different volumetric replacement percentages, such as 5%, 10%, 15%, and 20% have been considered for the present study. Since the specific gravity of LSP is lower than OPC, LSP content would have been higher on a weight basis mix design. Aggregate contents are designed considering Saturated Surface Dry (SSD) conditions. Table 3 presents the quantities of different materials in concrete mixes for five distinct combinations. C100L0 denotes no cement replacement, whereas C85L15 means 85% cement and 15% LSP.

A total of 90 cylinders is cast for conducting different mechanical and durability tests. The mold size for the cylinders is 100 mm in diameter x 200 mm in height. 15 beams with mold sizes of 100 mm x 100 mm x 500 mm are prepared for five different concrete mixes to evaluate the flexural strength at 28 days.

2.3 Test Procedure

A concrete mixer machine was used to mix the concrete ingredients. The LSP and cement are carefully blended by hand before being poured into the mixing device. Coarse aggregate was first put into the machine. Then sand, cement, and LSP mix, and water are added in that order. The mixer machine rotated appropriately to ensure proper mixing of the ingredients. For the slump test, freshly produced concrete is utilized. The slump value of concrete mixtures was measured using the ASTM C143 [40] standard. Specimens were stored in a moist room for the first 24 hours. After that, the samples were carefully demolded and placed in a temperature-controlled (23±2°C) curing tank.

The compressive strength test was performed using a 1500 kN capacity compression testing machine per ASTM C39 (2021). The load was applied at a rate of 0.25 MPa/s. Before testing, both surfaces of each cylinder were levelled using a grinder machine. The splitting tensile strength test was performed in the compression machine, following ASTM C496 (2017) at a loading rate of 0.2 MPa/s. The flexural strength of the concrete beams was evaluated in a 1000 kN capacity universal testing machine (UTM) following ASTM C78 (2022) at a displacement-controlled loading rate of 0.15 mm/min. Support-to-support distance was 300 mm, and the load was applied at 100 mm from the supports (Figure 3(a)).

The chloride ion penetrability of the concrete was determined by the surface resistivity test using a surface resistivity meter following the guidelines of AASHTO TP 95 (2011). After curing, the cylinders were kept outside to dry out before performing the surface resistivity test. The tip of the machine was then dipped in water before being placed against the cylinder to get the reading, and the data was obtained from all four sides of the cylinder by repeating the same procedure.

One cylinder from each combination was kept under 5 bar hydrostatic pressure for the water permeability test for 72 hours. BS EN 12390–8:2009 (2009) regulates the test procedure that involves injecting water under pressure into one surface of the specimen for a certain period, dividing the specimen perpendicular to the injected face, and measuring the depth of penetration visually. The hydrostatic pressure was applied at the centre from the bottom side of the cylinder by using a water permeability test apparatus (Figure 3(b)). The reading of permeability was manually measured from the divided cylinder.

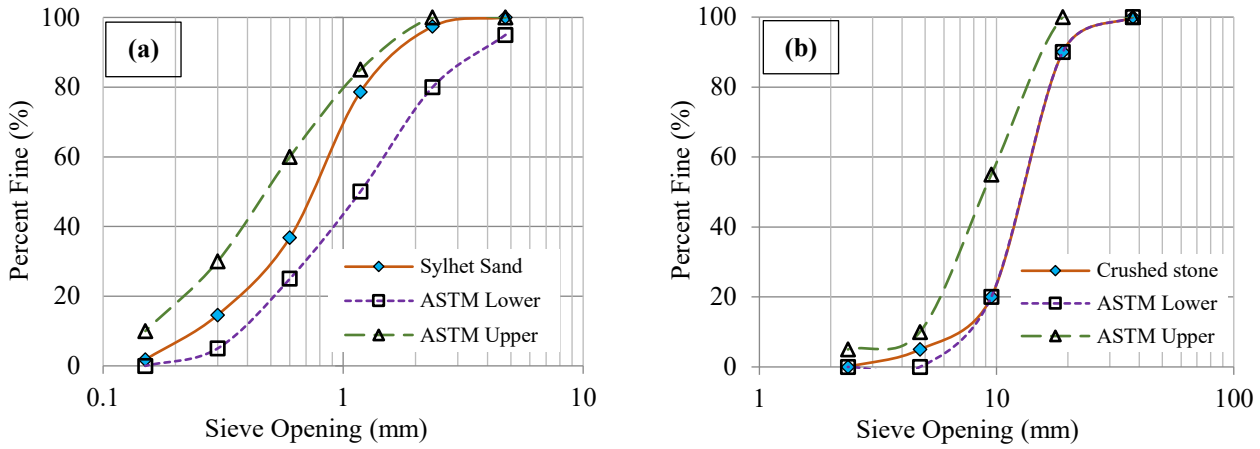

Figure 2: Gradation curves for (a) Fine aggregate and (b) Coarse aggregate

Table 3: The proportion of materials for one cubic meter of concrete mix

Batch Code	LSP replacement (%)	Water (kg)	Cement (kg)	LSP (kg)	FA (kg)	CA (kg)
C100L0	0	205	456.00	0.00	731.4	979.6
C95L5	5	205	433.20	22.80	729.6	979.6
C90L10	10	205	410.40	45.60	727.7	979.6
C85L15	15	205	387.60	68.40	725.9	979.6
C80L20	20	205	364.80	91.20	724.1	979.6

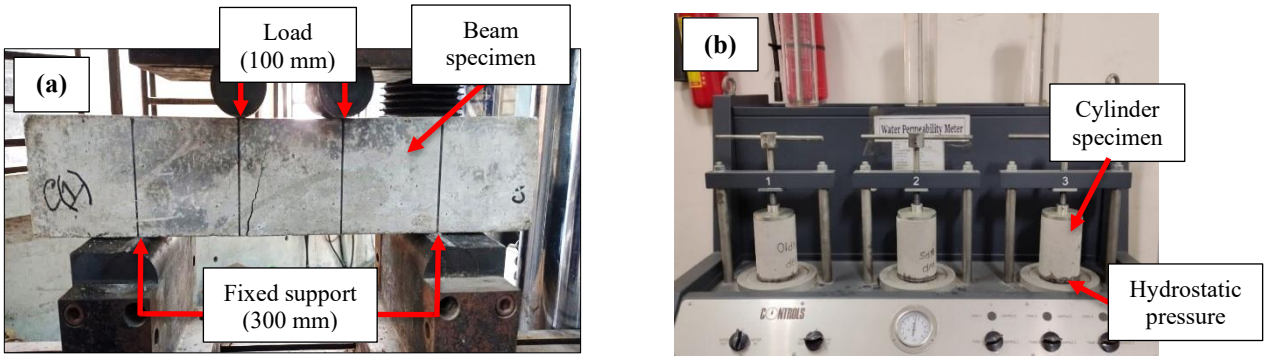

Figure 3: Test setup (a) Quasi-static flexural test (b) Water permeability test

3. RESULTS AND DISCUSSIONS

3.1 Workability

The slump value was measured immediately after the concrete was poured from the mixer machine to evaluate the workability. Figure 4 shows the slump value of all five concrete mixtures. Results show that the control combination had the lowest workability of the specimens under consideration in this investigation. Slump value increased with increasing LSP content, and the highest slump value was found for concrete with 20% LSP (C80L20). Slump value increases by 27%, 44%, 104% and 119% compared to the control sample for 5%, 10%, 15% and 20% LSP replacement, respectively.

The impacts of LSP on concrete workability are primarily due to the morphological influence, filler effect, and dilution effect. Since LSP is finer than the cement particles, the filler effect predominates in this case. LSP enhances workability by filling voids between larger particles, reducing water requirement, and improving the consistency of the concrete mix and ease of handling (Ratsarahasina *et al.*, 2022). When the particle size of LSP is equal to or larger than the particle size of cement particles, LSP demonstrates a diluting impact (D. Wang *et al.*, 2018a). Direct grinding of LSP enhances concrete flow values, mostly connected to the particles' surface morphology and fineness, increasing concrete flow values.

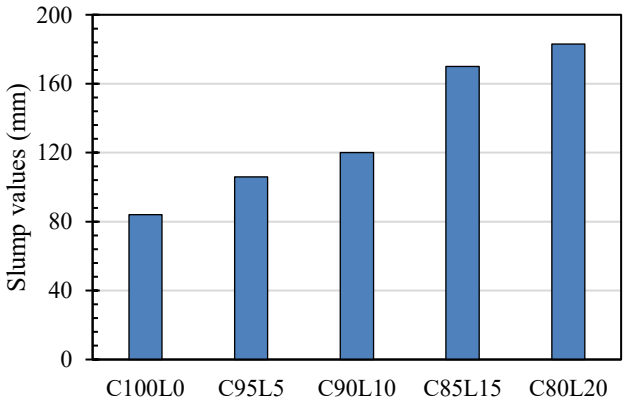

Figure 4: Slump value of different concrete mixtures

3.2 Compressive Strength

Figure 5 illustrates a summary of the compressive strength of concrete at 7, 28, and 56 days. Progressive growth in concrete strength with age for all combinations of concrete specimens has been observed. For example, the compressive strength of the control specimen differs by 12% from 28 days to 56 days. With the increasing percentage of LSP replacement, the compressive strength decreases initially and reaches a maximum of 10% LSP replaced concrete. A similar result was observed by Zhao *et al.* (2024) when sand was replaced by 10% LSP. However, beyond 10% LSP replacement, a decrease has been observed. The highest compressive strengths are 39.45 MPa and 44.28 MPa at 28 and 56 days, respectively, for 10% LSP replaced concrete (C90L10). As LSP enhances the pore structure of hardened concrete, the strength boosts up in later days (Yu *et al.*, 2014). At 28 days, strength increased by 1% for concrete with 10% LSP compared to the control specimen, but strength decreased by 5%, 16% and 18%, respectively, for concrete with 5%, 15% and 20% LSP. Compared to the control concrete specimen, strength increased by 1% at 56 days for concrete containing 10% LSP, but decreased by 4%, 11% and 17%, respectively for concrete with 5%, 15% and 20% LSP.

The result indicates that the inclusion of LSP decreases the compressive strength of concrete. The reason is the reduction of the hydraulically active clinker fraction of cement upon the LSP replacement (Sezer, 2012). At 10% LSP level, the compressive strength increases due to the nucleation effect of LSP. Beyond 15% replacement level, the dilution effect triggers, where the cement content is reduced, causing a slower hydration rate and potentially lowering the mechanical performance (A. H. Ahmed *et al.*, 2023). The less reactive calcite dilutes the more reactive cement when LSP replaces ordinary Portland Cement by more than 15%, resulting in reduced compressive strengths and physical changes (Benachour *et al.*, 2008; Dhir *et al.*, 2007). Also, the decrease in strength might be attributed to the reduced cementing qualities and an increase in non-cementing elements of the limestone fillers (Pliya & Cree, 2015). Liu and Yan (2010) reported from XRD analysis that LSP remains unhydrated at 28 days, even without having pozzolanic properties. The LSP used in this research was finer than the cement particle, and when a high amount of fine LSP was utilized to substitute cement, the LSP showed a dilution effect and decreased compressive strength. This pattern demonstrates that the beneficial filler and nucleation effects of LSP are effective up to an optimum replacement level, beyond which the dilution effect dominates and adversely affects concrete strength. At higher replacement levels, LSP mostly acts as an inert filler, which reduces the amount of reactive clinker and thereby lowers strength (Bonavetti *et al.*, 2003). Figure 6 depicts failure patterns, and in most cases, a diagonal fracture with no cracking through the ends is observed in cylinders. Samples with 5% LSP have columnar failure. Higher content than that results in a cone and shear crack.

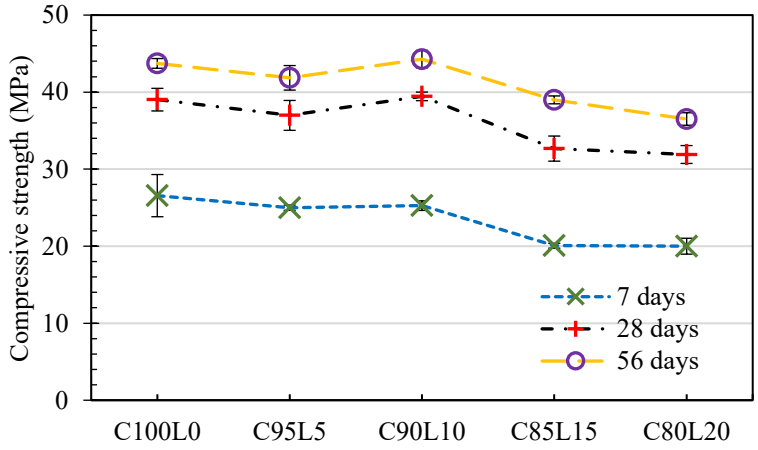

Figure 5: Compressive strength at 7, 28 and 56 days

(a) (b) (c) (d) (e)

Figure 6: Failure patterns of cylinders subjected to a compressive force at 56 days (a) C100L0, (b) C95L5, (c) C90L10, (d) C85L15, (e) C80L20.

3.3 Splitting Tensile Strength

Figure 7 represents the summary of the splitting tensile strengths of concrete at 7 and 28 days. The tensile strength of concrete has been observed to grow with age. As illustrated in Figure 7, the inclusion of LSP decreases concrete's tensile strength. For example, the tensile strength increases for 5% LSP at 7 days. However, for 10% LSP, it is almost the same as the control specimen and again drops by 21% and 14% for 15% LSP at 7 and 28 days, respectively, compared to the control mix. Tensile strength is the highest for 5% LSP for both 7 days and 28 days of curing. For 28 days, the highest strength is 3.49 MPa for 5% LSP. However, the increment of strength is not much compared to the control specimen, only 1.2%. Thus, adding LSP does not increase the strength by a noticeable amount. The addition of 10% LSP has a similar tensile strength as the specimen without any LSP. Although a slight increment is observed for 20% LSP at 7 days (19%) and 28 days (1%) compared to 15% LSP containing samples.

LSP serves as an inert filler element. Too much of that results in a poor fiber-matrix interface (Zhou *et al.*, 2010) and cementitious material's strain-hardening activity is harmed by an excessively weak interface (V. C. Li, 2003). A smaller dosage of LSP (up to 10%) optimizes the pore structures of aggregates and facilitates the early hydration of cement due to the filler and nucleation effects (Zhao *et al.*, 2024). At 15% LSP dosage, the dilution of cement dominates, which limits available clinkers for hydration in the matrix, causing a decrease in tensile strength. For these reasons, tensile strength decreases with the increment of the percentage of LSP. However, at a 20% dosage, LSP provides additional nucleation sites for calcium silicate hydrate (C-S-H) formation, which compensates for the dilution effect of cement to some extent. Thus, an increment in tensile strength is observed at more than 15% LSP level (Shi *et al.*, 2023).

From the failure patterns (Figure 8), it can be seen that vertical cracking occurred through both ends for up to 10% LSP content. The 15% and 20% LSP containing cylinders have horizontal cracks, which made them fail at lower tensile stress levels. Samples with 10% LSP also shows a few thin horizontal cracks. These horizontal cracks indicate that adding a higher amount of LSP increases the brittle behaviour of concrete.

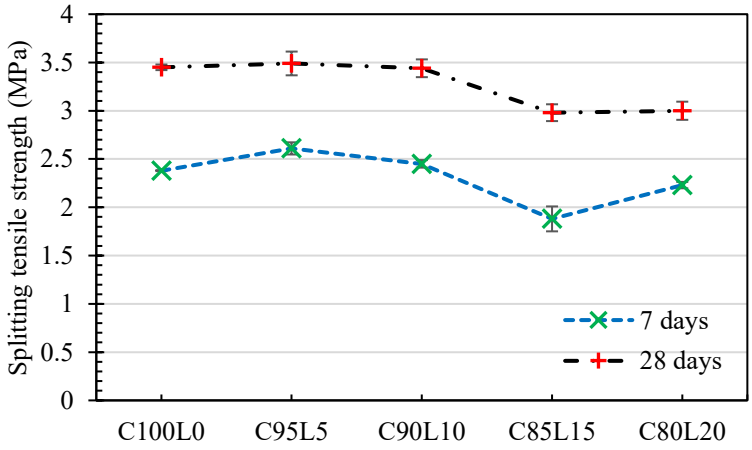

Figure 7: Influence of LSP on splitting tensile strength of concrete

(a) (b) (c) (d) (e)

Figure 8: Failure patterns of cylinders subjected to a tensile force at 28 days (a) C100L0, (b) C95L5, (c) C90L10, (d) C85L15, (e) C80L20.

3.4 Relationship between Compressive Strength and Splitting Tensile Strength

Several design codes refer to equations to calculate the tensile strength of concrete from the compressive strength values. However, these design codes do not take LSP into account. The experimental splitting tensile strength from this study is compared with the ACI 318-14 (2014), fib 2010 (2010), and Eurocode 2 (2005) equations, which are shown in Figure 9. The code equations overestimate the 7 days results and underestimate the 28 days results. LSP hydrates at a later days, thus its strength gain is slow. This

is why the inconsistency with the code occurs. ACI318-14, fib 2010, and Eurocode 2, respectively overestimate tensile strength up to 32%, 18% and 19% for 7 days and underestimates by up to 3%, 5% and 13% for 28 days. Thus, a new equation has been proposed by a machine learning approach using python programming language by adopting a linear regression model on the experimental data from this study along with other data from previous studies (Mohammed & Al-Numan, 2024; Ahmad *et al.*, 2022; Demirhan *et al.*, 2019; Hyun *et al.*, 2018; Kim *et al.*, 2018; Diab *et al.*, 2016; Nikbin *et al.*, 2014; Adel Mohammed *et al.*, 2010). The input features the percentage of LSP and compressive strength, and the outcome gives the prediction of tensile strength. Using a total of 50 datasets, 100000 iterations have been performed with a learning rate of 0.00000005 to reduce error (Figure 10(a)). R^2, RMSE, and MAE of the model have been found to be 0.547, 0.587 and 0.515, respectively. Considering the presence of LSP as supplementary cementitious material, Equation 1 has been proposed to predict the tensile strength from compressive strength.

$$\text{Splitting tensile strength} = 0.073f_c' - 0.013\text{LSP} \quad (1)$$

Where, f_c' = compressive strength and LSP = percentage of limestone powder. This equation has 12.67% accuracy, which means that the proposed equation is accurate and can be used for practical applications. The performance of the regression model has been evaluated using 10-fold cross-validation. The model achieved an average R^2 of 0.614±0.124, with RMSE and MAE values of 0.602±0.178 and 0.545±0.188, respectively, across the folds. Figure 10(b) shows the linear relation between compressive strength and splitting tensile strength obtained from the machine learning procedure.

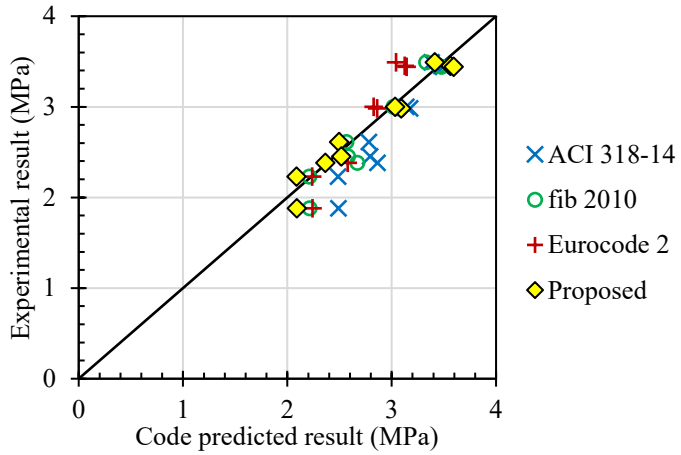

Figure 9: Comparison of experimental tensile strength data with various code-predicted data

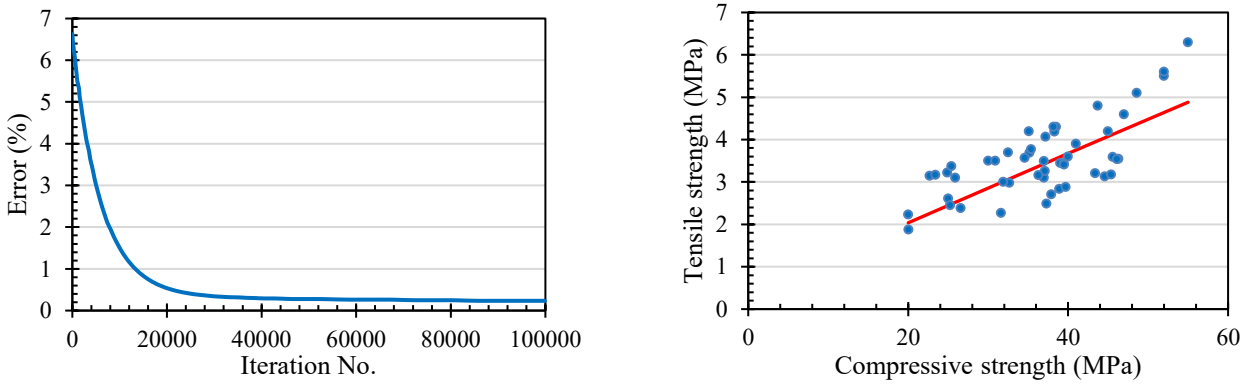

Figure 10: (a) Percentage of error vs. iteration plot and (b) Tensile strength and compressive strength dataset from previous studies

3.5 Flexural Behavior

The quasi-static flexural strength test data after 28 days of curing are presented in Table 4. The flexural stress initially increases by 5.5% and 6.4% for adding 5% and 10% LSP with cement, respectively. However, an increment of LSP amount decreases the flexural stress aftermath. Flexural stress is the highest for 10% LSP which is 10.36 MPa. The lowest flexural stress was observed for 20% LSP, where flexural stress decreased 1.2% and 9.6% for 15% and 20% LSP, respectively.

When used in place of cement, LSP mostly displays filler and diluting effects, which can densify the concrete microstructure and improve the interfacial transition zone between the cement paste and aggregates (Ratsarahasina *et al.*, 2022; Kępniak *et al.*, 2021; Liu & Yan, 2010). LSP also promotes the heteronucleation of cement hydration products on the limestone particles, further enhancing the cement matrix (Kępniak *et al.*, 2021). Hence, the use of LSP in place of up to 10% cement improves the flexural strength of concrete. Similar result is also observed by W. Li *et al.* (2015). When higher LSP content is used to replace more than 10% of cement, the cementing material content decreases, and the non-cementing component

Table 4 Flexural strength test results at 28 days.

Mix ID	First crack load (kN)	Maximum load (kN)	Deflection at maximum load (mm)	Flexural stress at maximum load (MPa)	Toughness (kN-mm)
C100L0	18.82	21.64	0.349	6.49	3.42
C95L5	20.72	22.83	0.398	6.85	4.31
C90L10	15.88	23.02	0.549	6.91	6.53
C85L15	16.33	21.37	0.616	6.41	5.40
C80L20	16.95	19.55	0.683	5.86	5.37

increases, which is responsible for the reduction of concrete flexural strength (D. Wang *et al.*, 2018b). There are residual LSP after filling up the spaces between aggregate particles. This governs the dilution effect, because of which the cement matrix becomes less dense, the hydration rate decelerates, which significantly lowers the amount of C-S-H formation (A. H. Ahmed *et al.*, 2023). This indicates that the volume of cement can be lowered up to 10% to increase the dimensional stability of concrete and reduce the risk of cracking without affecting strength. This is attributed to the filler effect of the LSP.

Figure 12 illustrates the Load-Deflection curves of the specimens. All the curves have the same pattern. Each curve is separated into three phases. The first stage begins at the loading point and finishes at the point where the slope of the curve first begins to vary. The first crack appears at this stage. At this point, the load-deflection curve seems to be linear, representing the uncracked beam. After increasing the load, the curve rises linearly to the highest point. The load vs deflection curve shows that the control specimen with 0% LSP has a straight elastic region up to the first crack load (18.82 kN), followed by a very short hardening region up to peak load (21.64 kN), indicating that it does not take much load after the first crack load appears. Adding LSP increases the elastic region and for this reason, it takes more time to fail compared to the control specimen. Following that, the beam bears no more stress, and an abrupt falling segment is visible. The concrete beam then fails like a brittle material. The deflection capacity also increases with higher LSP, as seen from Table 4. It is to be noted that although the 10% LSP level has the lowest first crack load among all the mixes (15.88 kN), failure load capacity of this mix is the highest (23.02 kN). This indicates that 10% LSP makes the concrete more brittle, allowing it to carry more flexural stress even after the first crack appears.

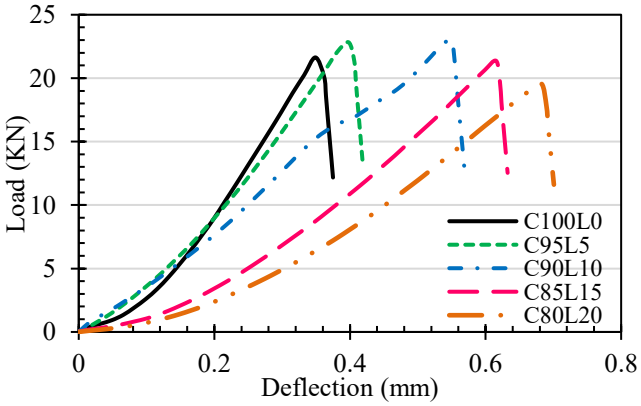

Figure 12: Load-deflection curves of concrete

The toughness index of each sample is determined using the load-deflection curves. From Table 4, it is seen that all the mixes containing LSP has a greater toughness value than the control mixes. The toughness index first starts to increase and is the highest for 10% LSP. After that, the toughness index starts to decrease with higher LSP amounts. The variation of toughness index is 26%, 90%, 58% and 57% respectively for 5%, 10%, 15% and 20% LSP compared to the control specimen. Therefore, it indicates that concrete with 10% LSP requires the most energy to fracture, and the control specimen requires the lowest energy to fracture. As the fracture toughness of a component with a specific length decreases, so does the component's capacity to bear load before cracking. For a given stress, however, when fracture toughness improves, a component may endure a longer crack before fracturing.

3.6 Chloride Ion Penetrability Test

The study of chloride permeability is an important factor that influences the durability of concrete. Figure 13 shows the surface resistivity of cylinders at different ages. These data are correlated to the penetrability standard according to AASHTO TP 95 (2011). Specific resistance values less than 12 are classified as high penetrability, and 12 KΩ-cm to 24 KΩ-cm are classified as moderate penetrability by this test method.

After 7 days of curing, all the samples have high penetrability, which migrates to a moderate level after 28 and 56 days of curing. The surface resistivity is the highest for specimens with 5% LSP and the lowest for 15% LSP content. Then the resistivity gradually decreases for 10% and 15% LSP. Surface resistivity increases by 8%, 4% and 3% for 5% LSP content after 7, 28, and 56 days of curing, respectively. According to D. Wang *et al.* (2018a), when a little quantity of fine LSP is used to substitute cement, it mostly works as a filler and reduces the chloride

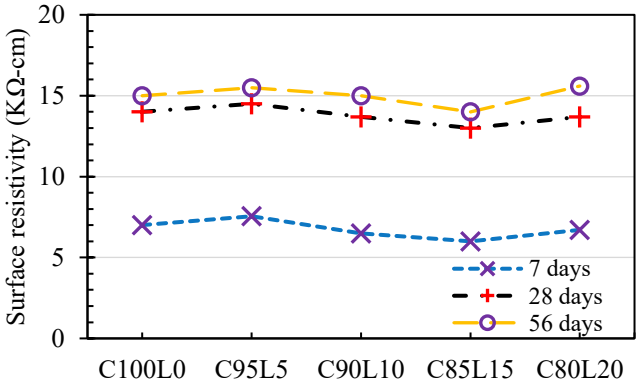

Figure 13: Chloride penetration of concrete with LSP

permeability of the concrete. This is why the samples with 5% LSP have the highest surface resistivity. With a longer curing period, concrete cylinders become more compacted and denser, and thus the surface resistivity increases for 28 and 56 days. The surface resistivity decreases by up to 14% for higher LSP content, which indicates higher chloride ion penetrability. A similar result was also observed by Hornain *et al.* (1995). Chloride ion penetrability is contingent upon the quantity and distribution of the pores. LSP refines the pore structure of concrete due to its filler and nucleation activities, and hence the chloride diffusion coefficient reduces as LSP concentration increases (D. Wang *et al.*, 2018a). Thus, the surface resistivity increases as well as the chloride ion penetrability decreases for the presence of LSP to an optimum level. Notably, at 56 days, a 4% increase in surface resistivity for 20% LSP is observed. This is attributed to the long-term pore refinement and matrix densification (Liu & Yan, 2010). This influences the surface resistivity at a higher replacement level of LSP.

3.7 Water Permeability Test

Figure 14 represents the permeability depth of concrete specimens under hydrostatic pressure and Figure 15 shows the depth of water in samples after the test. The permeability of the control specimen is 25 mm. Increasing the percentage of LSP reduces permeability. Similar trend was observed by L. G. Li and Kwan (2015) when cement was replaced by LSP. The water permeability is the highest for the control specimen. Then for all the combinations, permeability is lesser and the lowest for 20% LSP. The decrement variation is 12%, 24%, 28% and 36% respectively for 5%, 10%, 15% and 20% LSP compared to the control specimen. LSP improves the particle packing density of the concrete mix, which enhances compaction and reduces porosity (Ratsarahasina *et al.*, 2022). This densification results in a compact, less permeable microstructure, which in turn enhances the water permeability as well as the overall strength and performance of the concrete. The reduction in permeability also suggests a denser interfacial transition zone (ITZ), which narrows down the pathways for water ingress (Liu & Yan, 2010). This suggests that the inclusion of LSP not only reduces permeability but may also improve durability under aggressive environmental conditions.

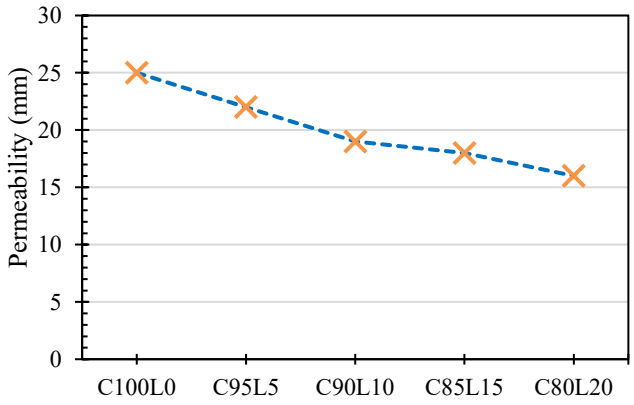

Figure 14: Water permeability of concrete with LSP

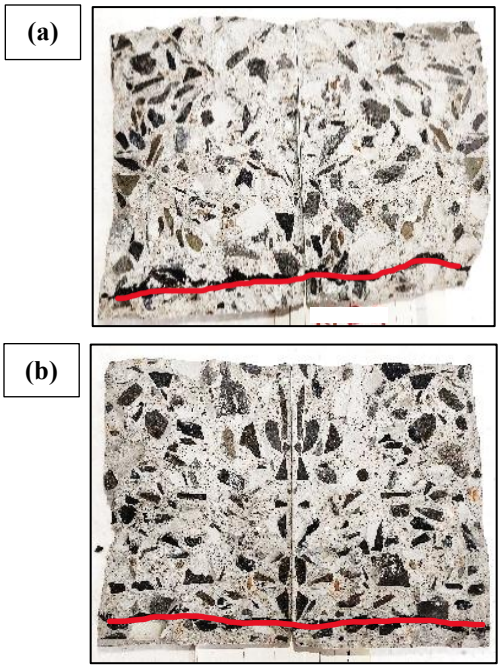

Figure 15: Samples after water penetration test (a)C100L0, (b) C80L20

4. CONCLUSIONS

The physical, mechanical, and durability features of LSP blended concrete are extensively investigated in this study. The findings may be best summed up:

i. Slump increases linearly with higher content of LSP. The filler effect of LSP makes the concrete flowable and thus increases workability.

ii. With the increasing percentage of LSP replacements, the compressive strength decreases initially and reaches a maximum of 10% LSP replaced concrete, 39.45 MPa, and 44.28 MPa at 28 and 56 days, respectively, due to the nucleation effect. The dilution effect caused by a higher percentage of LSP offsets the hydration process which reduces compressive strength for 15% and 20% LSP.

iii. With the addition of LSP, the splitting tensile strength does not vary significantly up to 10% replacement. After both 28 and 56 days of curing, the splitting tensile strength of the 10% LSP sample and the control sample are almost similar. Afterwards, tensile strength decreases. A smaller dosage of LSP optimizes the pore structure and facilitates the early hydration, which does not disadvantage the tensile strength. An equation has been proposed to predict the tensile strength of LSP mixed concrete using a machine learning approach.

iv. Maximum flexural strength is obtained for 10% percent LSP, which is 6.4% higher than the control specimen. The toughness index also has a similar trend, which increases by 90% for 10% LSP. Higher LSP content gradually reduces flexural strength. This happens because there are residual LSP after the optimum amount, which governs the dilution effect.

v. The water permeability and chloride ion penetrability gradually reduce with the addition of LSP. For 5% LSP content, the surface resistivity is the highest because a smaller amount of LSP works mostly as filler and produces a compact, less permeable microstructure, which enhances the water permeability and chloride ion penetrability of concrete. 10% LSP content gives a similar surface resistivity as the control specimen.

LSP blended concrete gives better mechanical and durability properties up to an optimum level. From the experimental results, it is consistent that 10% LSP has the best outcome in terms of mechanical and durability properties. Thus, 10% LSP can be considered as the optimum level to substitute Portland cement.

ACKNOWLEDGMENTS

The authors would like to thank MIST for providing the necessary facilities and technical support required to successfully conduct the experimental investigations of this study.

DATA AVAILABILITY STATEMENT

Datasets generated during the current study are available from the corresponding author upon reasonable request.

FUNDING DECLARATION

This research was financially supported by a start-up fund provided by the authors. Special thanks to Seven Rings Cement for partnering with the project.

ETHICS APPROVAL

This study is an engineering experimental investigation. The MIJST Research Ethics Committee has confirmed that formal ethical approval was not required.

ETHICS, CONSENT TO PARTICIPATE, AND CONSENT TO PUBLISH

Not applicable.

COMPETING INTERESTS

The authors declare that they have no competing interests.

AUTHOR CONTRIBUTIONS

Author 1: Md. Jahidul Islam- Writing – review & editing, Supervision, Methodology, Conceptualization, Funding acquisition, Formal analysis.

Author 2: Tasnia Ahmed- Data curation, Formal analysis, Software, Writing – original draft.

Author 3: Nishat Naila Meghna- Investigation, Data curation, Formal analysis, Writing – original draft.

Author 4: Ismat Abida- Investigation, Data curation.

Author 5: Nayeem Mohammad Mashfiq- Investigation, Data curation

ARTIFICIAL INTELLIGENCE ASSISTANCE STATEMENT

Portions of this manuscript were assisted by an artificial intelligence language model (ChatGPT, OpenAI). The tool was used solely for language editing, text refinement, and clarity improvement. All content, data interpretation, analysis, conclusions, and final decisions were generated, verified, and approved by the authors. The authors take full responsibility for the accuracy and integrity of the manuscript.

CONFLICT OF INTEREST DECLARATION

The authors declare that they have no conflicts of interest.

REFERENCES

AASHTO TP 95. (2011). Standard Method of Test for Surface Resistivity of Concrete's Ability to Resist Chloride Ion Penetration. *American Association of State Highway and Transportation Officials, Washington, DC*.

ACI 211.1. (1991). Standard Practive for Selecting Proportions for Normal, Heavyweight, and Mass Concrete. *American Concrete Institute, Farmington Hills, MI*.

ACI 211.7R-15. (2015). Guide For Proportioning Concrete Mixtures With Ground Limestone and Other Mineral Fillers. *American Concrete Institute, Farmington Hills, MI*.

ACI 318-14. (2014). Building Code Requirements for Structural Concrete and Commentary. *American Concrete Institute, Farmington Hills, MI*.

Adel Mohammed, Z., Burhan Abdurrahman, R., & Abdul Hakeem Hamed Ahmad, D. (2010). Influence of Limestone Powder as Partial Replacement of Cement on Concrete and the Effect of High Temperature on It. *Al-Rafidain Engineering Journal (AREJ), 18*(5), 24-34. doi:10.33899/rengj.2010.32863

Ahmad, I., Shen, D., Khan, K. A., Jan, A., & Ahmad, T. (2022). Evaluation of mechanical properties and environmental impact of using limestone powder in high-performance concrete. *Magazine of Concrete Research, 74*(24), 1280-1295. doi:10.1680/jmacr.21.00199

Ahmed, A. H., Nune, S., Liebscher, M., Köberle, T., Willomitzer, A., Noack, I., Butler, M., & Mechtcherine, V. (2023). Exploring the role of dilutive effects on microstructural development and hydration kinetics of limestone calcined clay cement (LC3) made of low-grade raw materials. *Journal of Cleaner Production, 428*, 139438. doi:https://doi.org/10.1016/j.jclepro.2023.139438

Ahmed, T., Bediwy, A., Azzam, A., Elhadary, R., El-Salakawy, E., & Bassuoni, M. T. (2024). Utilization of Novel Basalt Fiber Pellets from Micro- to Macro-Scale, and from Basic to Applied Fields: A Review on Recent Contributions. *Fibers, 12*(2), 17. doi:https://doi.org/10.3390/fib12020017

Ahmed, T., Bediwy, A., & Islam, M. J. (2025). Durable and sustainable nano-modified basalt fiber-reinforced composites for elevated temperature

applications. *Journal of Building Engineering, 108*, 112865. doi:https://doi.org/10.1016/j.jobe.2025.112865

Amran, M., Makul, N., Fediuk, R., Lee, Y. H., Vatin, N. I., Lee, Y. Y., & Mohammed, K. (2022). Global carbon recoverability experiences from the cement industry. *Case Studies in Construction Materials, 17*, e01439. doi:https://doi.org/10.1016/j.cscm.2022.e01439

Araf, S., Shahjalal, M., Ahmed, T., Juthi, S., Rahman, S., & Islam, M. (2023). *Mechanical and Durability Properties of Induction Furnace Slag and Recycled Aggregate Concrete.* Paper presented at the 2nd International Conference on Advances in Civil Infrastructure and Construction Materials, 26-28 July 2023, MIST, Dhaka, Bangladesh.

ASTM C33. (2023). *Standard Specification for Concrete Aggregates*. Paper presented at the ASTM International, West Conshohocken, PA.

ASTM C39. (2021). Standard Test Method for Compressive Strength of Cylindrical Concrete Specimens. *ASTM International, West Conshohocken, PA*.

ASTM C78. (2022). Standard Test Method for Flexural Strength of Concrete (Using Simple Beam with Third-Point Loading). *ASTM International, West Conshohocken, PA*.

ASTM C150. (2022). Standard Specification for Portland Cement. *ASTM International, West Conshohocken, PA*.

ASTM C187. (2023). Standard Test Method for Amount of Water Required for Normal Consistency of Hydraulic Cement Paste. *ASTM International, West Conshohocken, PA*.

ASTM C188. (2023). Standard Test Method for Density of Hydraulic Cement. *ASTM International, West Conshohocken, PA*.

ASTM C191. (2021). Standard Test Method for Time of Setting of Hydraulic Cement by Vicat Needle. *ASTM International, West Conshohocken, PA*.

ASTM C204. (2024). Standard Test Methods for Fineness of Hydraulic Cement by Air-Permeability Apparatus. *ASTM International, West Conshohocken, PA*.

ASTM C496. (2017). Standard Test Method for Splitting Tensile Strength of Cylindrical Concrete Specimens. *ASTM International, West Conshohocken, PA*.

Barbhuiya, S., Kanavaris, F., Das, B. B., & Idrees, M. (2024). Decarbonising cement and concrete production: Strategies, challenges and pathways for sustainable development. *Journal of Building Engineering, 86*, 108861. doi:https://doi.org/10.1016/j.jobe.2024.108861

Barbhuiya, S., Nepal, J., & Das, B. B. (2023). Properties, compatibility, environmental benefits and future directions of limestone calcined clay cement (LC3) concrete: A review. *Journal of Building Engineering, 79*, 107794. doi:https://doi.org/10.1016/j.jobe.2023.107794

Benachour, Y., Davy, C. A., Skoczylas, F., & Houari, H. (2008). Effect of a high calcite filler addition upon microstructural, mechanical, shrinkage and transport properties of a mortar. *Cement and Concrete Research, 38*(6), 727-736. doi:https://doi.org/10.1016/j.cemconres.2008.02.007

Bonavetti, V., Donza, H., Menéndez, G., Cabrera, O., & Irassar, E. F. (2003). Limestone filler cement in low w/c concrete: A rational use of energy. *Cement and Concrete Research, 33*(6), 865-871. doi:https://doi.org/10.1016/S0008-8846(02)01087-6

BS EN 12390–8:2009. (2009). The Standard for Testing hardened concrete - Depth of Penetration of Water under pressure. *British Standards Institution, UK*.

Celik, K., Hay, R., Hargis, C. W., & Moon, J. (2019). Effect of volcanic ash pozzolan or limestone replacement on hydration of Portland cement. *Construction and Building Materials, 197*, 803-812. doi:https://doi.org/10.1016/j.conbuildmat.2018.11.193

Chen, J., Kwan, A., & Jiang, Y. (2014). Adding limestone fines as cement paste replacement to reduce water permeability and sorptivity of concrete. *Construction and Building Materials, 56*, 87-93.

Chen, J., Kwan, A., & Jiang, Y. (2014). Adding limestone fines as cement paste replacement to reduce water permeability and sorptivity of concrete. *Construction and Building Materials, 56*, 87–93. doi:10.1016/j.conbuildmat.2014.01.066

Demirhan, S., Turk, K., & Ulugerger, K. (2019). Fresh and hardened properties of self consolidating Portland limestone cement mortars: Effect of high volume limestone powder replaced by cement. *Construction and Building Materials, 196*, 115-125. doi:https://doi.org/10.1016/j.conbuildmat.2018.11.111

Dhir, R., Limbachiya, M., McCarthy, M., & Chaipanich, A. (2007). Evaluation of Portland limestone cements for use in concrete construction. *Materials and structures, 40*(5), 459-473. doi:https://doi.org/10.1617/s11527-006-9143-7

Diab, A. M., Abd Elmoaty, A. E. M., & Aly, A. A. (2016). Long term study of mechanical properties, durability and environmental impact of limestone cement concrete. *Alexandria Engineering Journal, 55*(2), 1465-1482. doi:https://doi.org/10.1016/j.aej.2016.01.031

EN, B. S. (2000). 197-1, Cement-Part 1: Composition, specifications and conformity criteria for common cements. *British Standards Institution*.

Eurocode 2. (2005). EN 1992-1-1, Design of Concrete Structures – Part 1–1: General Rules and Rules for Buildings. *Thomas Telford, London, UK*.

fib 2010. (2010). fib Model Code for Concrete Structures. *International Fedaration for Structural Concrete*.

Gesoğlu, M., Güneyisi, E., Kocabağ, M. E., Bayram, V., & Mermerdaş, K. (2012). Fresh and hardened characteristics of self compacting concretes made with combined use of marble powder, limestone filler, and fly ash. *Construction and Building Materials, 37*, 160-170.

Hornain, H., Marchand, J., Duhot, V., & Moranville-Regourd, M. (1995). Diffusion of chloride ions in limestone filler blended cement pastes and mortars. *Cement and Concrete Research, 25*(8), 1667-1678. doi:https://doi.org/10.1016/0008-8846(95)00163-8

Hyun, J. H., Lee, B. Y., & Kim, Y. Y. (2018). Composite Properties and Micromechanical Analysis of Highly Ductile Cement Composite Incorporating Limestone Powder. *Applied Sciences, 8*(2), 151. doi:https://doi.org/10.3390/app8020151

Islam, M. J., Ahmed, T., Imam, S. M. F. B., Islam, H., & Shaikh, F. U. A. (2023a). Comparative study of carbon fiber and galvanized iron textile reinforced concrete. *Construction and Building Materials, 374*, 130928. doi:https://doi.org/10.1016/j.conbuildmat.2023.130928

Islam, M. J., Ahmed, T., Salehin, M. R., Sakib, M. S., Shariar, M. S., & Hossain, M. (2023b). Physical, Mechanical, and Durability Properties of Concrete with Class F Fly Ash. *MIST INTERNATIONAL JOURNAL OF SCIENCE AND TECHNOLOGY, 11*(2). doi:10.47981/j.mijst.11(02)2023.430(27-41)

Kępniak, M., Woyciechowski, P., & Franus, W. (2021). Transition Zone Enhancement with Waste Limestone Powder as a Reason for Concrete Compressive Strength Increase. *Materials, 14*, 7254. doi:10.3390/ma14237254

Kim, Y.-J., Leeuwen, R. v., Cho, B.-Y., Sriraman, V., & Torres, A. (2018). Evaluation of the Efficiency of Limestone Powder in Concrete and the Effects on the Environment. *Sustainability, 10*(2), 550. doi:https://doi.org/10.3390/su10020550

Li, L. G., & Kwan, A. K. (2015). Adding limestone fines as cementitious paste replacement to improve tensile strength, stiffness and durability of concrete. *Cement and Concrete Composites, 60*, 17-24. doi:https://doi.org/10.1016/j.cemconcomp.2015.02.006

Li, P. P., Brouwers, H. J. H., Chen, W., & Yu, Q. (2020). Optimization and characterization of high-volume limestone powder in sustainable ultra-high performance concrete. *Construction and Building Materials, 242*, 118112. doi:https://doi.org/10.1016/j.conbuildmat.2020.118112

Li, V. C. (2003). On engineered cementitious composites (ECC) a review of the material and its applications. *Journal of Advanced Concrete Technology, 1*(3), 215-230.

Li, W., Huang, Z., Cao, F., Sun, Z., & Shah, S. P. (2015). Effects of nano-silica and nano-limestone on flowability and mechanical properties of ultra-high-performance concrete matrix. *Construction and Building Materials, 95*, 366-374. doi:https://doi.org/10.1016/j.conbuildmat.2015.05.137

Lin, W.-T., Cheng, A., & Černý, R. (2020). Effect of limestone powder on strength and permeability of cementitious mortars. *MATEC Web of Conferences, 322*, 01009. doi:10.1051/matecconf/202032201009

Liu, S., & Yan, P. (2010). Effect of limestone powder on microstructure of concrete. *Journal of Wuhan University of Technology-Mater. Sci. Ed., 25*(2), 328-331. doi:10.1007/s11595-010-2328-5

Lothenbach, B., Le Saout, G., Gallucci, E., & Scrivener, K. (2008). Influence of limestone on the hydration of Portland cements. *Cement and Concrete Research, 38*(6), 848-860. doi:https://doi.org/10.1016/j.cemconres.2008.01.002

Mahi, M. S. H., Ridoy, T., Faiag, M., & Sheikh, M. (2025). Limestone Powder in Concrete Mixes: A Review of Mechanical Enhancements. *Smart and Green Materials, 2*, 11-21. doi:10.70028/sgm.v2i1.25

Meddah, M. S., Lmbachiya, M. C., & Dhir, R. K. (2014). Potential use of binary and composite limestone cements in concrete production. *Construction and Building Materials, 58*, 193-205.

Meghna, N. N., Abida, I., Mashfiq, N. M., Ahmed, T., Karim, M. R., & Islam, M. J. (2025, 2025//). *Influence of Mechanical and Durability Properties of Concrete with Limestone Powder.* Paper presented at the Proceedings of the Canadian Society for Civil Engineering Annual Conference 2023, Volume 6, Cham.

Mohammed, B. K., & Al-Numan, B. S. (2024). Effectiveness of Limestone Powder as a Partial Replacement of Cement on the Punching Shear Behavior of Normal- and High-Strength Concrete Flat Slabs. *Sustainability, 16*(5), 2151. doi:https://doi.org/10.3390/su16052151

Nikbin, I. M., Beygi, M. H. A., Kazemi, M. T., Vaseghi Amiri, J., Rabbanifar, S., Rahmani, E., & Rahimi, S. (2014). A comprehensive investigation into the effect of water to cement ratio and powder content on mechanical properties of self-compacting concrete. *Construction and Building Materials, 57*, 69-80. doi:https://doi.org/10.1016/j.conbuildmat.2014.01.098

Pliya, P., & Cree, D. (2015). Limestone derived eggshell powder as a replacement in Portland cement mortar. *Construction and Building Materials, 95*, 1-9.

Ratsarahasina, D. M., Ratsimbazafy, H. M., Robisonarison,

G. J., Randrianirainy, H. P. B., & Ramaroson, J. D. D. (2022). Etudes Des Influences Du Filler Calcaire Sur La Maniabilité Et Le Retrait Du Béton. *International Journal of Progressive Sciences and Technologies, 31*(1), 11. doi:10.52155/ijpsat.v31.1.4088

Sezer, G. İ. (2012). Compressive strength and sulfate resistance of limestone and/or silica fume mortars. *Construction and Building Materials, 26*(1), 613-618.

Shi, J., Wu, Z., Zhuang, J., Zhang, F., Zhu, T., & Li, H. (2023). Synergistic Effects of SAP, Limestone Powder and White Cement on the Aesthetic and Mechanical Properties of Fair-Faced Concrete. *Materials, 16*(21), 7058.

Vance, K., Kumar, A., Sant, G., & Neithalath, N. (2013). The rheological properties of ternary binders containing Portland cement, limestone, and metakaolin or fly ash. *Cement and Concrete Research, 52*, 196-207. doi:https://doi.org/10.1016/j.cemconres.2013.07.007

Wang, D., Shi, C., Farzadnia, N., Shi, Z., & Jia, H. (2018a). A review on effects of limestone powder on the properties of concrete. *Construction and Building Materials, 192*, 153-166. doi:https://doi.org/10.1016/j.conbuildmat.2018.10.119

Wang, D., Shi, C., Farzadnia, N., Shi, Z., Jia, H., & Ou, Z. (2018b). A review on use of limestone powder in cement-based materials: Mechanism, hydration and microstructures. *Construction and Building Materials, 181*, 659-672. doi:https://doi.org/10.1016/j.conbuildmat.2018.06.075

Wang, Q., Yang, J., & Chen, H. (2017). Long-term properties of concrete containing limestone powder. *Materials and Structures, 50*(3), 168. doi:10.1617/s11527-017-1040-8

Wang, X.-Y. (2020). Optimal mix design of low-CO2 blended concrete with limestone powder. *Construction and Building Materials, 263*, 121006. doi:https://doi.org/10.1016/j.conbuildmat.2020.121006

Yu, R., Spiesz, P., & Brouwers, H. J. H. (2014). Effect of nano-silica on the hydration and microstructure development of Ultra-High Performance Concrete (UHPC) with a low binder amount. *Construction and Building Materials, 65*, 140-150. doi:https://doi.org/10.1016/j.conbuildmat.2014.04.063

Zhao, L., He, T., Niu, M., Chang, X., Wang, L., & Wang, Y. (2024). Effect of Limestone Powder Mixing Methods on the Performance of Mass Concrete. *17*(3), 617.

Zhou, J., Qian, S., Beltran, M. G. S., Ye, G., van Breugel, K., & Li, V. C. (2010). Development of engineered cementitious composites with limestone powder and blast furnace slag. *Materials and structures, 43*(6), 803-814. doi:https://doi.org/10.1617/s11527-009-9549-0